

Validation of a Micro-Controller for Oxygen Control in the NICU

---

A Thesis

presented to

the Faculty of the Graduate School

at the University of Missouri-Columbia

---

In partial fulfillment

of the requirement of the degree

Master of Science

---

By

Zachary S. Jones

Dr. Roger Fales, Advisor

May 2023

The undersigned, appointed by the Dean of the Graduate School, have examined the thesis entitled

Validation of a Micro-Controller for Oxygen Control in the NICU

presented by Zachary S. Jones,

a candidate for the degree of Master of Science,

and hereby certify that in their opinion it is worthy of acceptance.

---

Professor Roger Fales

---

Professor Craig Kluever

---

Professor James Noble

## **ACKNOWLEDGMENTS**

I would first like to thank Dr. Roger Fales for accepting me on as a research assistant and being my advisor. His continuous patience, support, and mentorship throughout my master's studies has been wonderful. He has always been very knowledgeable and generous with his time. I would also like to thank Dr. Craig Kluever, and Dr. James Noble for serving on my committee. I really appreciate your comments and time. Also, would like to thank Dr. John Pardalos and all the nursing staff for their support and assistance in running a clinical trial.

I would also like to thank my research colleagues Brooke Runge, Nate Hardy, Tyler Schuster, Andrew Luebbert, and Sarah Muller. Throughout my graduate research, each one of these individuals contributed time and knowledge to get these devices built, tested, and ready for a clinical trial.

Furthermore, I would like to thank my friends and family for their support and encouragement throughout my college career, without them I would not have gotten this far. Lastly, I wanted to thank my sister-in-law, Tori Jones, for reading through my thesis and suggesting edits over the last few weeks.

## TABLE OF CONTENTS

Acknowledgements.....	iii
Table of Contents .....	iv
Table of Figures .....	vi
Table of Tables .....	vii
Abstract.....	viii
1. Introduction.....	1
1.1 Background.....	1
1.2 Motivation.....	2
1.3 Literature Review.....	2
1.3.1 Previous Work at the University of Missouri — Columbia .....	2
1.3.2 Previous work with sbRIO-9628 .....	6
1.4 Contributions.....	6
1.5 Goals and Objectives .....	7
1.6 Outline of Thesis.....	7
2. Methods.....	8
2.1 Design Requirements .....	8
2.1.1 Case.....	8
2.1.2 Logic Board .....	8
2.1.3 Power Supply.....	9
2.1.4 Screen.....	9
2.1.5 Automatic Blend Valve Assembly.....	9
2.2 Analysis and Specifications .....	10
2.2.1 Case .....	10
2.2.2 Logic Board .....	11
2.2.3 Power Supply.....	13
2.2.4 Touchscreen User Interface .....	14
2.2.5 Automatic Blend Valve Assembly.....	15
2.3 Implementation .....	16
2.4 Testing.....	18

2.5 Redesigns .....	19
3. Results.....	21
3.1 Design Results .....	21
3.2 Lab Testing Results.....	22
3.3 Clinical Trial Results .....	27
3.4 Discussion.....	30
4. Conclusion and Future Work .....	33
References.....	35

## Table of Figures

Figure 1.1 First-generation prototype control board .....	5
Figure 2.1 Internal component layout with case dimensions (Wires, switches, and connectors excluded) .....	10
Figure 2.2 The left side shows the case dimensions along with the rear panel layout, while the right side shows the front panel layout .....	11
Figure 2.3 Dimensional specification for the sbRIO-9627 and sbRIO-9628 [17] .....	13
Figure 2.4 Schematic drawing of the SOLA SCP30 S12-DN [19].....	14
Figure 2.5 Dimensional layout of the touchscreen interface [20].....	15
Figure 2.6 Motor and encoder assembly .....	16
Figure 2.7 New knob with full assembly .....	16
Figure 2.8 Internal layout of the case.....	17
Figure 2.9 Wiring diagram.....	18
Figure 2.10 Full simulation testing setup.....	19
Figure 3.1 Prototype device .....	22
Figure 3.2 Manual/Auto switch transition over an hour .....	23
Figure 3.3 Manual/Auto switch transition over an hour SpO <sub>2</sub> .....	24
Figure 3.4 Manual/Auto switch transition over an hour FiO <sub>2</sub> .....	24
Figure 3.5 Simulation desaturation and feeding test.....	26
Figure 3.6 Simulation desaturation and feeding test SpO <sub>2</sub> .....	26
Figure 3.7 Simulation desaturation and feeding test FiO <sub>2</sub> .....	27

## Table of Tables

Table 2.1 Requirements for Logic Board.....	12
Table 3.1 Simulation results, percentage of time spent in each SpO <sub>2</sub> range in manual and automatic.....	25
Table 3.2 Simulation results, percentage of time spent in manual and automatic in each FiO <sub>2</sub> ranges.....	25
Table 3.3 Clinical results from Subject 1-3, percentage of time patients are in a safe range .....	28
Table 3.4 Average of the subjects, percentage of time spent in manual and automatic in each FiO <sub>2</sub> ranges .....	28
Table 3.5 Average of the subjects, percentage of time spent in each SpO <sub>2</sub> range in manual and automatic from the SpO <sub>2</sub> Setpoint .....	28
Table 3.6 Patient one FiO <sub>2</sub> range in both modes in percent on time in each .....	29
Table 3.7 Patient one SpO <sub>2</sub> range from the SpO <sub>2</sub> Setpoint in both modes in percent on time in each .....	29
Table 3.8 Patient two FiO <sub>2</sub> range in both modes in percent on time in each .....	29
Table 3.9 Patient two SpO <sub>2</sub> range from the SpO <sub>2</sub> Setpoint in both modes in percent on time in each .....	29
Table 3.10 Patient three FiO <sub>2</sub> range in both modes in percent on time in each .....	30
Table 3.11 Patient two SpO <sub>2</sub> range from the SpO <sub>2</sub> Setpoint in both modes in percent on time in each .....	30

## ABSTRACT

Respiratory support is required for premature infants who are born with underdeveloped lungs and insufficient surfactant production, which is the cause of respiratory distress syndrome (RDS). The lack of surfactant inhibits the lung's ability to inflate properly, which is required for ventilation. With this, the peripheral oxygen saturation ( $SpO_2$ ) of the neonates admitted into the Neonatal Intensive Care Unit (NICU), requires nurses to adjust the fraction of inspired oxygen ( $FiO_2$ ) that the blend valve is supplying. The desired range of the  $SpO_2$  is 88%–95% blood oxygen saturation levels, and this is monitored using existing sensors in the NICU. Nurses rely on these sensors to make manual adjustments of the  $FiO_2$  in the range of 21%–100% oxygen, depending on the needs of the neonate. This is done to avoid hypoxemia and hyperoxemia. Keeping the  $SpO_2$  in the predetermined range is a strenuous task for nurses, who often have fluctuating workloads providing care to multiple patients simultaneously. Exacerbating this is the variation of the neonate's  $SpO_2$ , which makes it difficult to keep within the target range. With the understanding of the currently used device and desired improvements, the research team at the University of Missouri — Columbia has developed an automatic oxygen controller to improve upon previous prototypes. Also, the team is conducting further lab and clinical trials to analyze the performance benefits of the improvements made to the device and to evaluate the manufacturability of the device using design for manufacturing methods (DFM). The design and implementation of the automatic oxygen control system was created with the improved  $FiO_2$  blend valves assembly designed by Pierce combined with new electrical hardware for expandability and reliability while using the same control algorithm as the previous prototype.

# 1. Introduction

## 1.1 Background

Premature infants are commonly born with underdeveloped lungs that frequently lead to RDS because of the lack of pulmonary surfactants. Up to 60% of mild-to-moderate RDS patients require a mechanical ventilator [5]. Continuous positive airway pressure (CPAP) or humidified high-flow nasal cannula (HNFC) are used in respiratory therapy to treat RDS. Both practices use a mechanical blend valve to adjust the  $FiO_2$ .  $FiO_2$  is the concentration of oxygen in a gas mixture. Currently, nurses do this manually to keep the neonate in a safe range — between 87%–93% — until the neonate has matured. The  $FiO_2$  is then increased to 91%–99%. This range is given because if the neonate stays too high, a state of hyperoxia occurs; this causes damage to the retinal tissue and can lead to blindness. But if the neonate stays too low, hypoxia occurs, which causes brain damage [8-10]. At this time, the  $FiO_2$  is manually adjusted by nurses for both CPAP and HNFC, and the levels are set and adjusted based on vital signs and trained nurses' judgment. An automated device that controls the  $FiO_2$  level in response to the  $SpO_2$  level would lessen the nurses' workload in the NICU while keeping the neonate in the desired range for a longer period. While an initial prototype succeeded, there were desired improvements. So, a second prototype device is designed, validated, and tested with both the improvements and the ability to replicate easily for manufacturing. This paper will explain the device's design, validation, and testing outside of the NICU, along with the beginning of clinical trials.

## **1.2 Motivation**

The motivation behind designing, validating, and testing a new prototype is to further improve upon the original design of the first prototype to improve the quality-of-care nurses provide to premature neonates. These improvements involved changing the internal design and hardware and implementing more serial interfaces for communication that the first prototype did not have. These changes also improve the device's manufacturability and make it easier to adapt it for future work. This is done using common manufacturing practices when designing the new prototype and laying out the internal hardware to improve the wiring layout for a clean, easy-to-follow, and to troubleshoot the new design.

## **1.3 Literature Review**

### **1.3.1 Previous Work at the University of Missouri — Columbia**

Researchers at the University of Missouri — Columbia (UMC) started working on solutions to control the oxygen saturation levels of neonates in the NICU more than a decade ago. Kiem one of the researchers on the project worked on the estimation systems of dynamic fuzzy logic, continuous parameter-estimating extended Kalman filter, and discrete parameter-estimating extended Kalman filter to develop an adaptive controller based on the discrete extended state observer and parameter-estimating extended Kalman filter estimation system [1-3]. Before Kiem's work, Krone had analyzed the relationship between  $SpO_2$  and  $FiO_2$  developing a first-order transfer function model. Krone showed that the  $FiO_2$ , heart rate (HR), and respiratory rate (RR) influenced the oxygenation of the blood [4,5]. With this knowledge, he created four different models showing  $SpO_2$  responses to changes in  $FiO_2$  [4,5]. The models are

the neural network, fuzzy logic, updating transfer function, and dynamic transfer function models [4,5].

When testing these models, Krone found the dynamic transfer function model to be the most accurate in modeling SpO<sub>2</sub> for a prolonged period [4,5]. Following the work done by Kiem and Krone, Quigley worked on developing a novel control system for regulating the SpO<sub>2</sub> in neonates. Quigley's work on the development of the H-infinity synthesis method to derive multiple controllers to achieve performance and stability for a larger range of parametric uncertainty in the model only a few years after Krone developed a dynamic transfer function model[6]. Work done by Alkurawy in analyzing the use of PI, PID, model predictive controller, robust control with PID, and robust control with model predictive controller to ensure stability and minimize settling time to reach an accurate output would help implement the  $\mu$  – synthesis controller in controlling the oxygen percentage in the FiO<sub>2</sub> and the performance specifications [7]. The results from his work showed that the robust controller with model predictive controller displayed the best performance for a system with larger ranges of modeling parameters. [7].

Faqeeh later developed a non-clinical investigation into the device's performance using a neonatal respiratory model (hardware-in-the-loop-test) [8,9,10]. This model is still used to test the device's performance. Belke's research followed and focused on developing a parameter uncertainty model for the dynamics of oxygen desaturation recovery events and comparing it with classical methods of uncertainty modeling [11]. A few years later, Hou developed a new automatic oxygen controller designed from the previous controller design concept. The second-generation adaptive controller was designed based on simulations of the actual system and the centroids of the stability. With the performance regions being the target of the controller gains setting [12,13]. Non-clinical tests were conducted to evaluate the performance of the new control

algorithm design before it was applied to real clinical tests [12,13]. Following this, Dutton worked on polynomial system identification modeling and adaptive model predictive control of arterial oxygen saturation in premature infants [14]. Pierce followed with redesigning the mechanical interface utilizing the existing  $\text{FiO}_2$  valve design while maintaining the same look and feel, reaching a desired response time for the valve position of one second, and allowing for repeatable manufacturing cycles of the interface [15].

Figure 1.1 shows the hardware of the first prototype. This system utilizes a sbRIO-9632. This board has an NI9870E modular interface for RS-232 communication, along with two NI 9505E modules as motor drivers. RS-232 communicates between data terminal equipment and data communications equipment using binary data exchange. This design ultimately was used in a pilot study with six infants admitted to the NICU that were less than or equal to 30 weeks gestational age or less than or equal to 1500 grams at birth who were on HFNC or CPAP and did not have congenital heart disease at the time of the study.

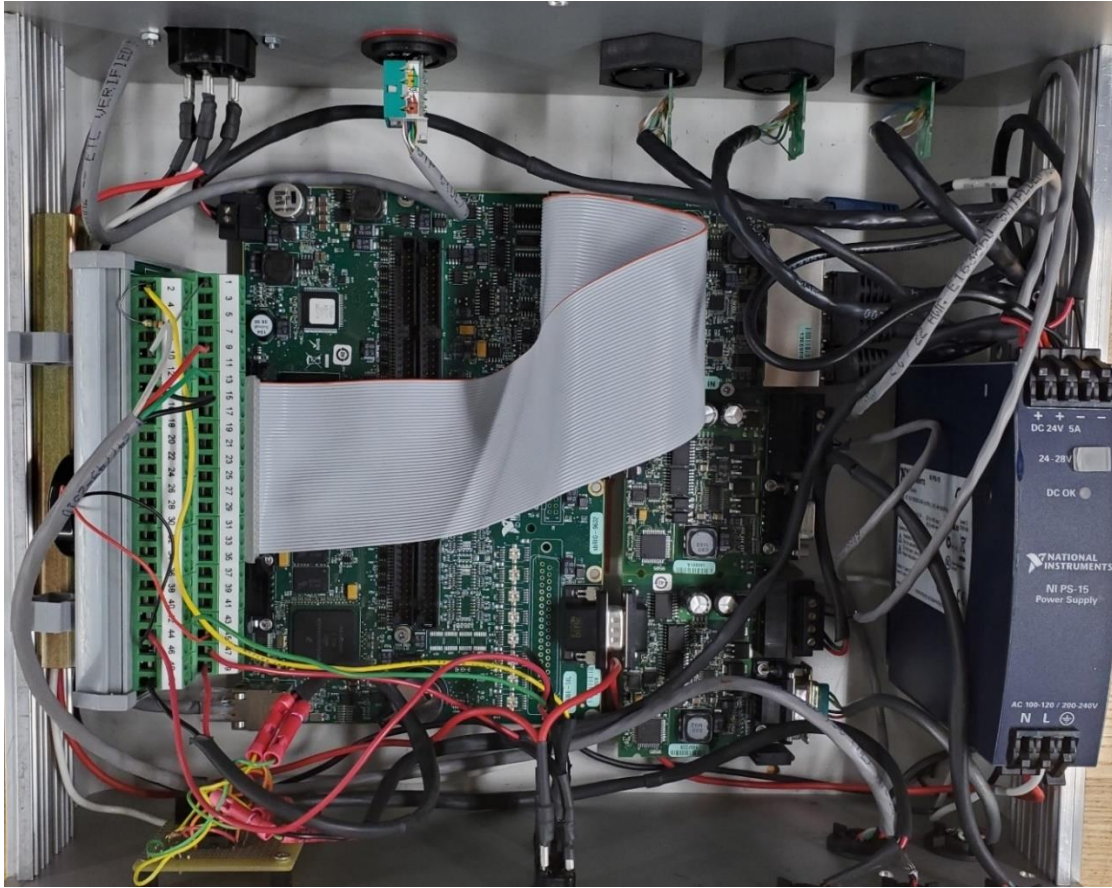


**Figure 1.1 First-generation prototype control board.**

The first-generation automatic oxygen control system uses the controller designed by Krone and Kiem [1-5]. Quigley later redesigned the automatic blend valve assembly to simplify the interface [6]. Hou Xuefeng then created the second-generation oxygen controller algorithm that would be run on the same system. With the new design of the algorithm, along with the development of the second-generation automated blend valve controller, the original single-board controller (CompactRIO) needed to allow the use of RS-485 communication and to support the touchscreen user interface to display parameters along with live data. This would lead to the elimination of the buzz motor and flow motor to simplify the controller. RS-485 is a specification defining the electrical interface and physical layer for point-to-point communication of electrical devices. The use of the control system originally developed by Kiem

and later adapted by Hou is still used to operate the new automated blend valve controller with improved control for both the position and speed of the motor, which is discussed by Pierce [15]. The implementation of the new blend valve system into the first prototype system was unsuccessful. A new CompactRIO was required to implement the encoder and motor. The encoder used in the redesign communicates via RS-485, which the current state of the first prototype did not support. Digital I/O is used to direct the motor driver as needed to achieve the required  $\text{FiO}_2$ . A motor driver is used to control the rotations per minute (rpm), direction, and state of the motor.

### **1.3.2 Previous work with sbRIO- 9628**

The single-board controller (sbRIO) has been used in another medical device research. CompactRIO was used for data acquisition and processing in million frames per second (Mfps) standalone X-ray detector for time-resolved experiments. The controller runs Linux-RT using the dual-core CPU and the field-programable gate array (FPGA) control to process the information from the UFXC32k hybrid pixel detectors and the Spartan-6 LX45. The Spartan is a second FPGA card. Using a 1 Gbps Ethernet connection allowed the system to stream up to 1.2 Mfps in burst mode and 70 thousand frames per second (kfps) is possible in zero-dead time mode [16].

### **1.4 Contributions**

This research produced a new control unit to combine the controller designed by Hou with Pierce's new interface design. The prototype had both a screen interface and the redesigned blend valve assembly while using the existing control algorithm developed by Hou. The prototype needed a more compact, reliable, and durable design that is simpler for the end users. Another contribution is lab and clinical testing results used to verify the design.

## **1.5 Goals and Objectives**

The goal of this work was to create a reliable device for use in testing an automatic oxygen control algorithm in a clinical trial in the NICU. The objectives of this work were to develop a prototype that implemented new electronic hardware (CompactRIO, digital and analog I/O, motor driver, and power supply) while being able to connect all the external interfaces (Spacelabs, oxygen analyzer, encoder, motor, power, power switch, automatic and manual control switch, and the screen). Another objective was to complete lab and clinical tests.

## **1.6 Outline of Thesis**

- Chapter 1 includes the background, motivations, literature review, contributions, goals, and objectives.
- Chapter 2 presents the design requirements of the new prototype, the requirements of the components, and the design of the non-clinical tests used to verify the device.
- Chapter 3 discusses why components were chosen, how they were implemented, and the results from non-clinical tests and during the clinical trial. It will also discuss the non-clinical tests and data from the first three clinical subjects with the prototypes.
- Chapter 4 concludes the research and covers future work.

## **2. Methods**

In this chapter, the design requirements of the new prototype are presented along with the performance results from lab testing. The new design requirements include new hardware components, more durability and reliability, and a more compact design.

### **2.1 Design Requirements**

As presented in Chapter 1, the first prototype was good for developing different blend valve assemblies, testing control algorithms, and collecting data. Nevertheless, the device needed to be more compact, reliable, durable, and simpler for the end users.

#### **2.1.1 Case**

The enclosure needs to be able to house the electronics, control board, digital and analog breakout board, power supply, and motor drivers. The case exterior needed to be adaptable both for connectors to pass through and for the structure required to mount on a standard medical IV pole.

#### **2.1.2 Logic Board**

The logic board requirements are to have RS-232, RS-485, digital and analog I/O, network interface ports, future expandability, and to be more reliable and durable for future updates to the firmware. It needs to be able to compute the control  $\text{FiO}_2$  from the  $\text{SpO}_2$  that is coming from Spacelabs, the  $\text{FiO}_2$  being measured from the oxygen analyzer, the comparison of the heart rate and pulse rate, and the flow of the air. During this the absolute encoder is sending its position to the board over RS-485 communication so that the algorithm knows its position and

can adjust it accordingly. This is done while the user touch interface is being updated with live data over RS-232.. It also needed to be able to store every data point every five seconds.

### **2.1.3 Power Supply**

The power supply needs to be an AC-to-DC converter that meets the requirements of the logic board, motor driver, encoder, switch indicator light, and user interface screen. A DC voltage reducer regulator step-down can be used if devices require voltage that is lower than that of the power supply.

### **2.1.4 Screen**

The screen needs to be a durable touchscreen interface that is easy to read and capable of communicating over serial to reliably show updated HR, PR, RR, SpO<sub>2</sub>, and FiO<sub>2</sub> numbers for the nurses to read and interact with reliably. It also needs a built-in alarm and the ability to input the max FiO<sub>2</sub> along with the delivery system of HNFC or CPAP. It needs to allow the setting of flow rate and SpO<sub>2</sub> Setpoint during operation. Finally, it needs a shutdown button to turn the device off.

### **2.1.5 Automatic Blend Valve Assembly**

This assembly designed by Pierce needs a one-second response time for valve position, a repeatable manufacturing cycle, the same look and feel for the end user, and using as much of the existing blend valve as possible. It also requires an absolute adjustment range from a feedback encoder allowing for precise adjustment in the range of 21-100% oxygen. Finally, the assembly requires a bump-resistant knob to prevent accidental adjustments.

## 2.2 Analysis and Specifications

### 2.2.1 Case

The case from the first prototype was desired because the case is durable, easy to acquire, compact, and meets the requirements in Sec. 2.1.1. The case layout fits all the required hardware and allows wiring pass-through. Figure 2.1 shows the dimensions and layout of the case, which leaves space to run wires. Figure 2.2 covers the wiring connector's design. Holes are cut out to prevent the connector from turning inside the panels. Each connector has a notch in the circular connector to lock it in the panel. This also allows for the connectors to be orientated the same throughout the case.

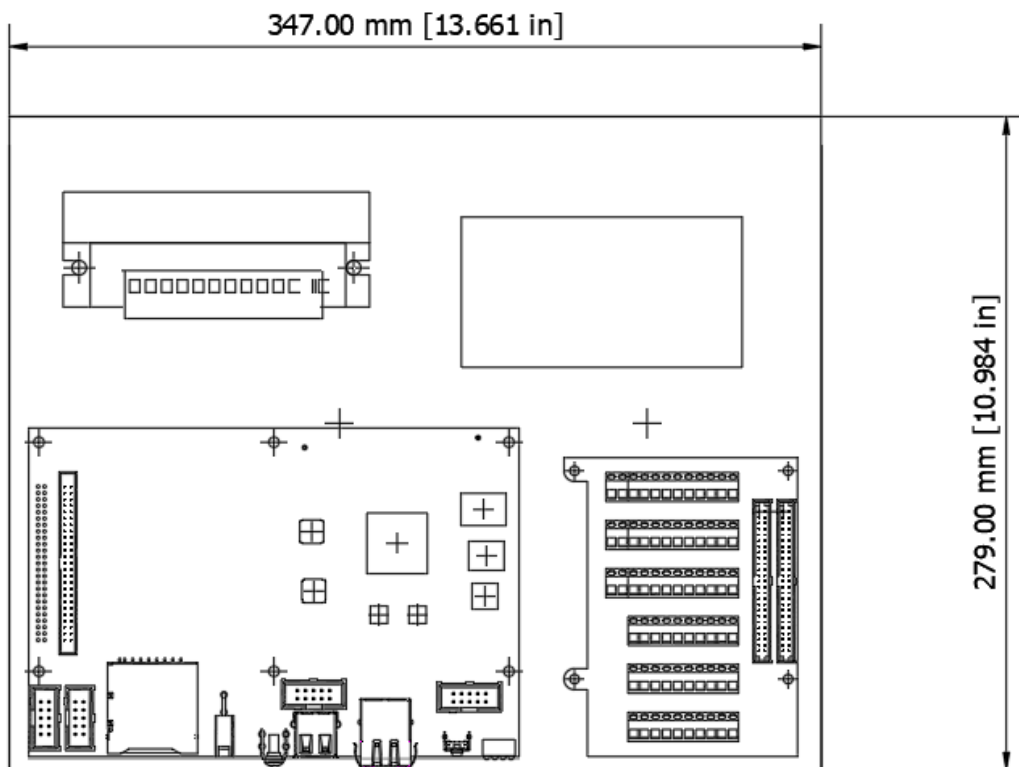


**Figure 2.1 Internal component layout with case dimensions (Wires, switches, and connectors excluded).**

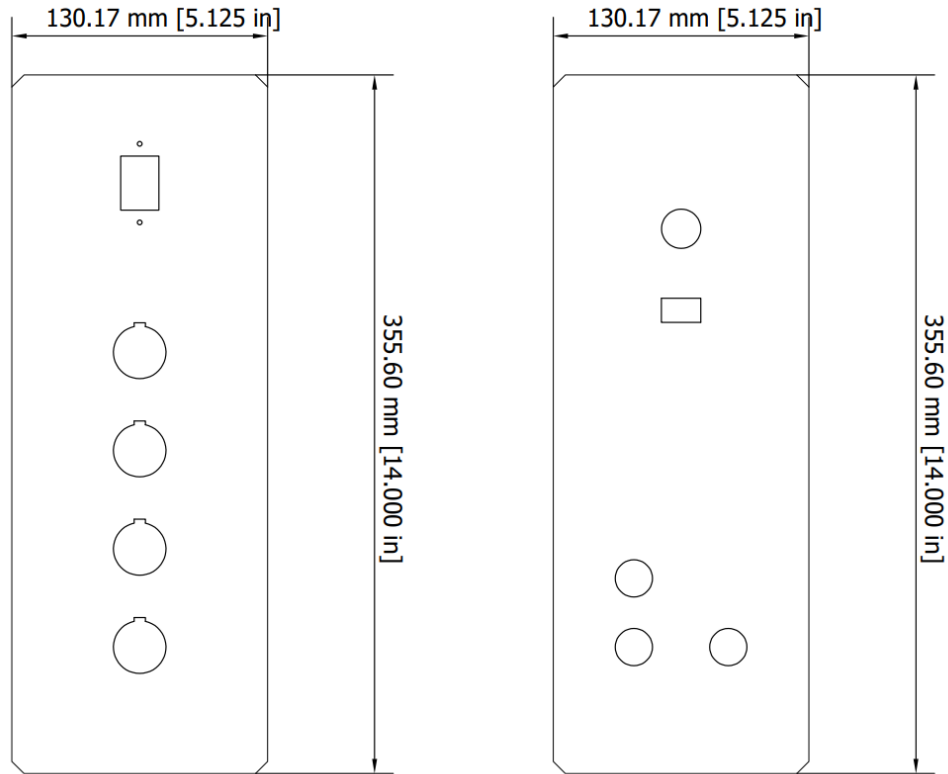


**Figure 2.2 The left side shows the case dimensions along with the rear panel layout, while the right side shows the front panel layout.**

### **2.2.2 Logic Board**

For the logic board to be implemented into the system, it must have RS-232, RS-485, digital and analog I/O, network interface ports, future expandability, and more reliability and durability. To meet these requirements, two logic boards designed by National Instruments were acquired. There are only a few differences in the boards. One runs off an Intel Atom processor, and the other runs off an ARM processor, so their respective chipsets are slightly different. In addition, one supports USB-C, while the other supports USB-A. Their basic manuals are almost identical, so both were ultimately tested.

The design and layout of both boards are the same and use the dimensions from the specification sheet in Fig. 2.3 [17]. Both have the same power requirements and number of ports for RS-232, RS-485, digital and analog I/O, and Ethernet. The boards also support 5-volt power from an attached mezzanine board. The attached mezzanine board can also add additional RS-232 and RS-485 ports. The max power consumption of the logic board is 55W with a 9V-30V rating.

**Table 2.1 Requirements for Logic Board**

<b>Description</b>	<b>Ports</b>	<b>Baud Rate</b>	<b>Data Bits</b>	<b>Parity</b>
Screen	RS-232	115200	8	None
Oxygen Analyzer	RS-232	2400	8	Odd
Spacelabs	RS-232	9600	8	None
Encoder	RS-485	115200	8	None
Digital/Analog I/O	3 DIO 4 AI 2AO	N/A	N/A	N/A

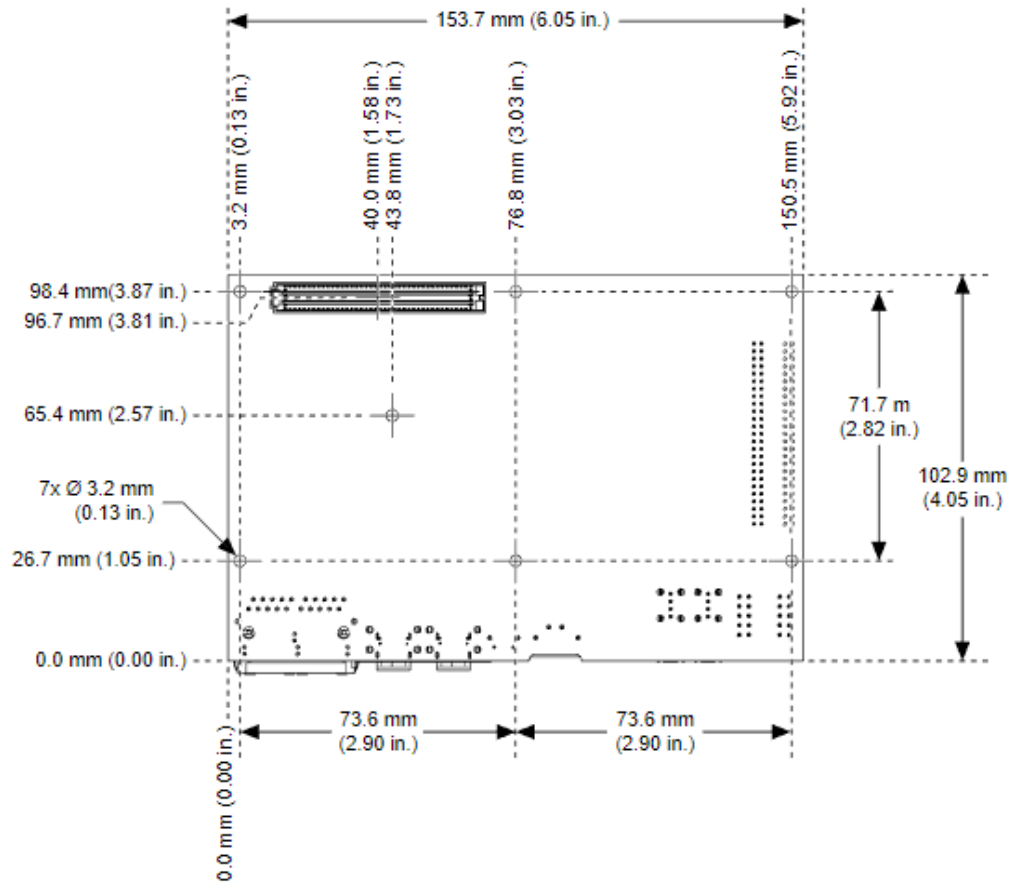


**Figure 2.3 Dimensional specification for the sbRIO-9627 and sbRIO-9628 [17].**

### 2.2.3 Power Supply

The logic boards' power requirements were examined with the need for a reliable AC-to-DC converter that meets the requirements of the logic board, motor driver, encoder, and user interface screen. A power converter that outputs 12 volts at 2.5 amps was selected because both boards have an input voltage of 9 V to 30 V DC, which is the same for the motor driver.

A SOLA SCP30 S12-DN was selected for its compact form, which meets the requirements of the logic board and motor driver. Figure 2.4 shows a diagram of the power supply. The unit is rated for 12 volts at 2.5 amps and greater than 75% efficiency.[19]

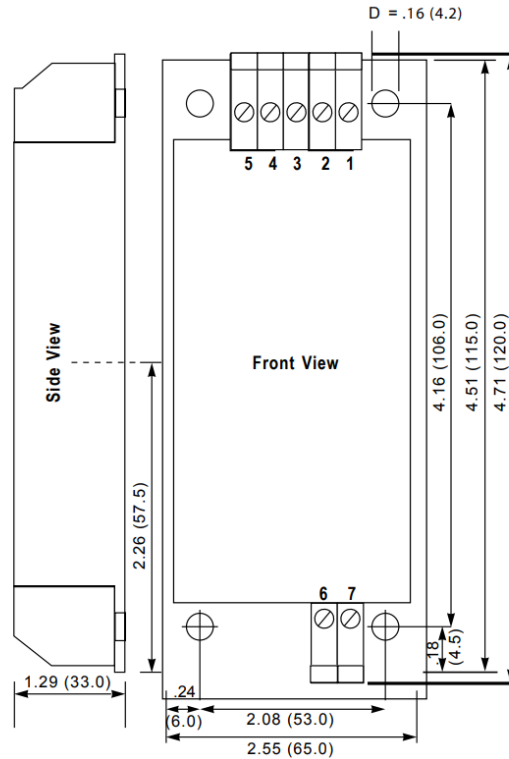


**Figure 2.4 Schematic drawing of the SOLA SCP30 S12-DN [19].**

## 2.2.4 Touchscreen User Interface

The touchscreen user interface for end users should be durable and easy to read, with a built-in alarm and reliable communication over serial. These requirements were met with a 4.3-inch touchscreen with serial communication over RS-232 and a power requirement of 5 volts.

Specifications for the Reach Technology 4.3" Standard display module meet the requirements and needs of this prototype. The screen has three serial ports, RS-232/3.3 V CMOS support, and a durable touchscreen along with power requirements of 5 volts and a max current requirement of 400 mA. The layout of the back of the touchscreen in Fig. 2.5 shows where the three serial interfaces are located. Each serial interface is designed to deliver the 5-volt power from the logic board to power the screen [20].

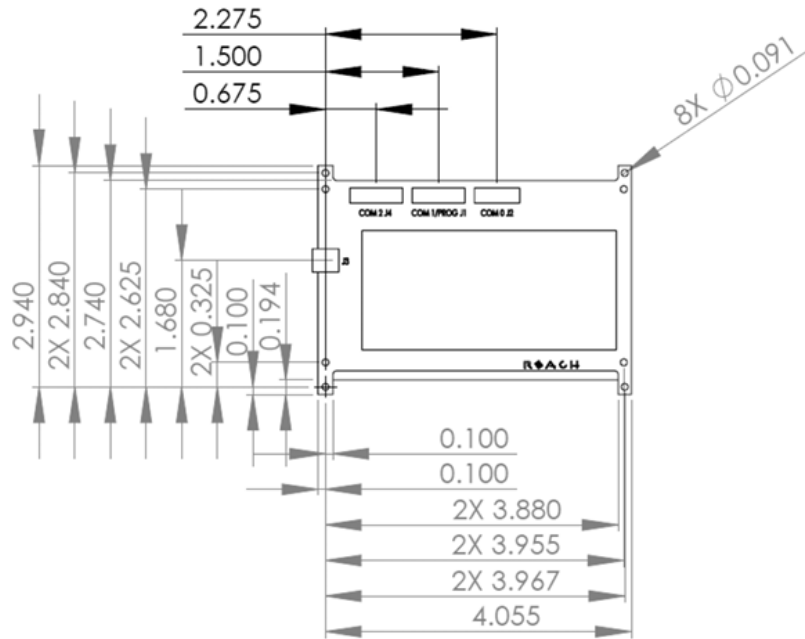


**Figure 2.5 Dimensional layout of the touchscreen interface [20].**

### **2.2.5 Automatic Blend Valve Assembly**

A full analysis of the automatic blend valve assembly can be read in Pierce's thesis [15]. The overall design uses a stepper motor with an inline absolute encoder. This combination of components allows for precise operation of the blend valve. The redesign of the blend valve assembly did not take into consideration the bend radius of the metal used to construct the new housing which caused a quarter inch out of alignment for the motor shaft and blend valve. Files were used to make sharper internal corners in the housing, and the back bracket was redesigned to align the center points better, which brought the design back into alignment. Finally, the blend valve assembly needed a bump-resistant knob on the new knob assembly. The original faceplate of the blend valve assembly was used to match the look of the original device, but a new knob design was used. Figure 2.6 shows the motor and encoder assembly, while the front full assembly is shown in Fig. 2.7.

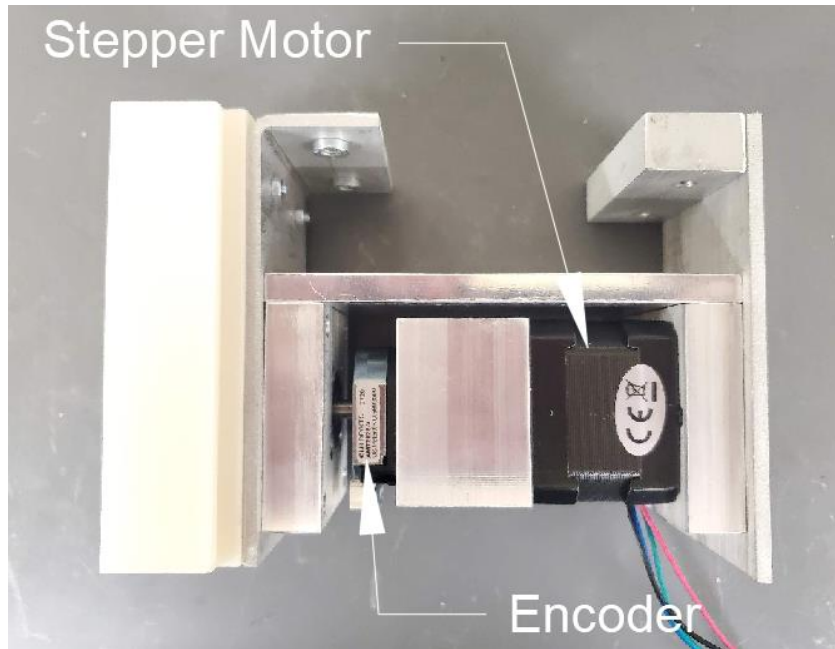


**Figure 2.6 Motor and encoder assembly.**



**Figure 2.7 New knob with full assembly.**

### **2.3 Implementation**

Assembly of these components started with fabricating the case parts so that each component had enough room to run wires through the case. The hole pattern in Fig. 2.1 is used to

attach all the internal components to the case. Figure 2.7 shows the component and wiring layout of the case, with a full wiring diagram in Fig. 2.8.

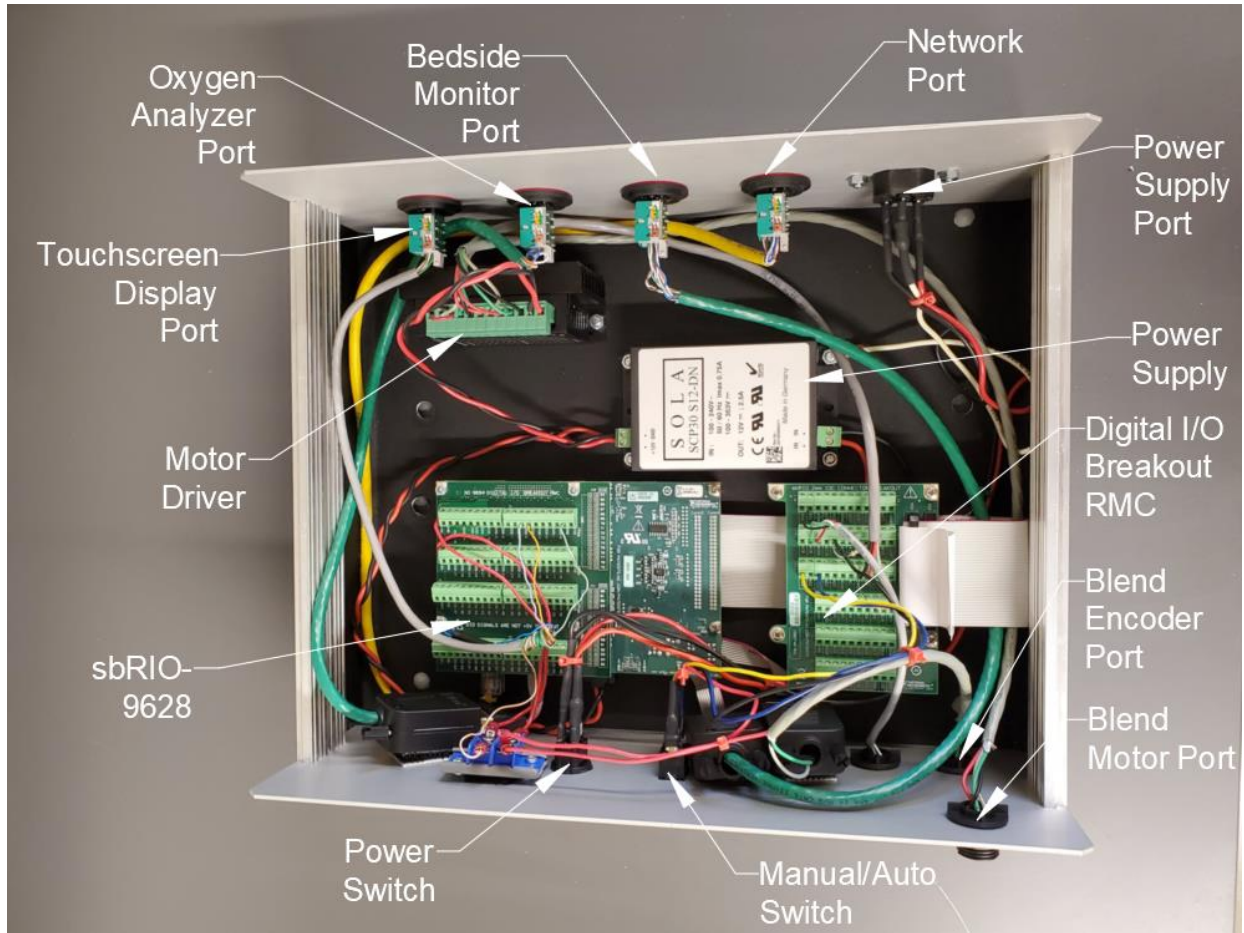


**Figure 2.8 Internal layout of the case.**



within the respiratory model [8-10]. The three different control factors are  $G_p$  and  $\tau$  to determine the response of the  $SpO_2$  after adjusting the  $FiO_2$ , as well as the levels of desaturation events represented by disturbances [12,13]. Both Faqeeh and Hou go into more detail about the design and implementation of the system. Figure 2.9 shows the setup of the device for the simulated testing.

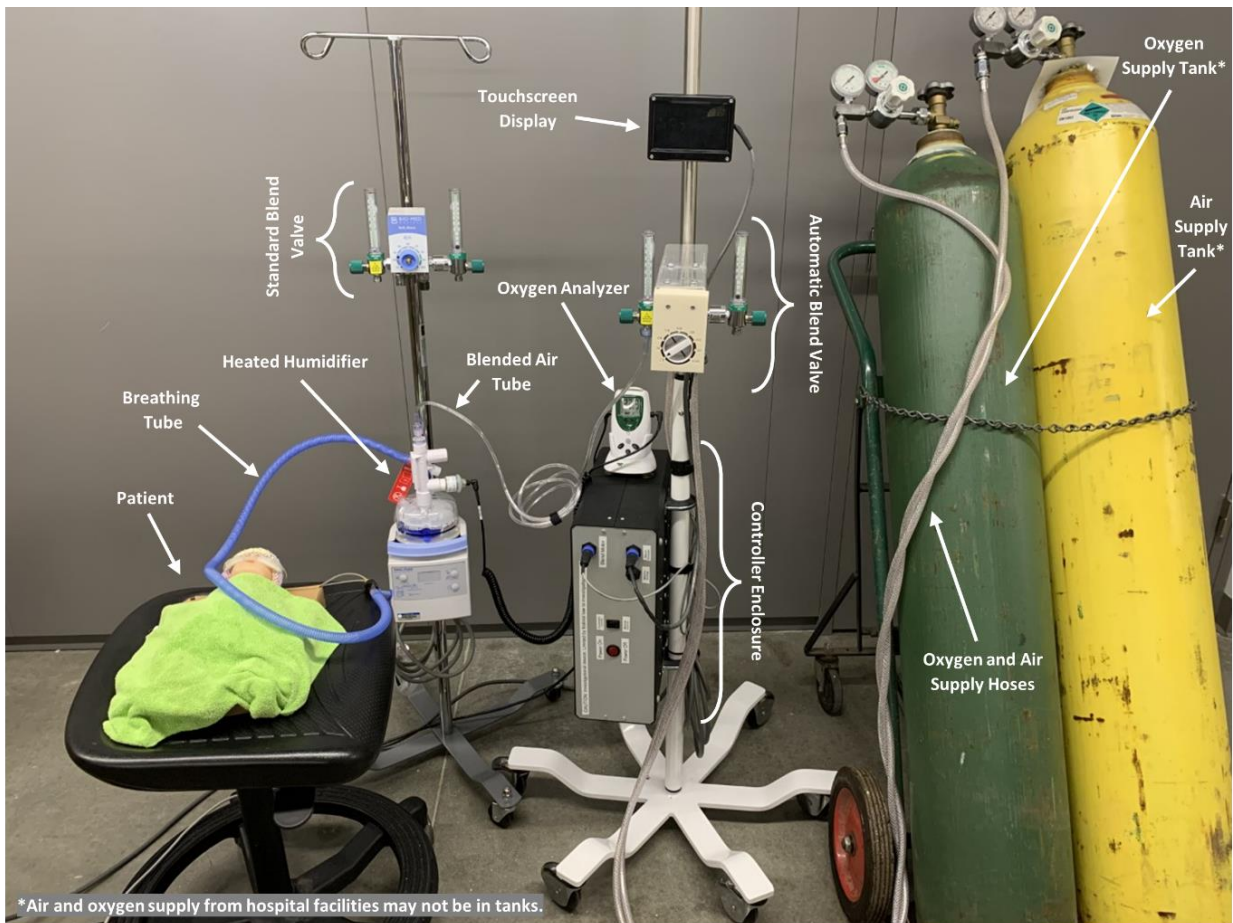


**Figure 2.10 Full simulation testing setup.**

## 2.5 Any Redesigns

Throughout the development of the device, several obstacles arose. These included manual/auto switch flipping without the switch position being changed, instability in the signals sent to the motor driver, alignment issues on the blend valve assembly, a redesign on the knob

used to operate the blend valve, and failure of the RS-485 on the logic board. With each of these issues, the system was tested and retested to validate that these problems were solved. The manual/auto switch required a pull-down resistor to prevent the terminal from building up a charge to 5-volts, which signaled to the system that the switch had been flipped. With the motor driver, a similar issue appeared, which caused the motor to change directions over a long period of time. Adding a pull-down resistor on each channel allowed for a cleaner signal to be sent to the motor driver. Finally, a component on the original sbRIO-9627 failed, which required a replacement. The replacement had a faulty RS-485, so only the sbRIO-9628 was tested.

### 3. Results

#### 3.1 Design results

Two test devices using the new design and components are currently being used in a clinical trial. Findings show that both the sbRIO-9627 and sbRIO-9628 work in this use case. However, receiving two 9628 boards and two 9627 boards with faulty RS-485 led to extensive testing of only the 9628. After the redesign of the blend valve assembly, the binding of the shaft coupler was nonexistent, which allowed for a smooth turn of the system, just like the original device. Following the implementation of the pull-down resistor, the system no longer built up enough charge to make a false positive result. Adding a pull-down resistor on the digital signals being sent to the motor driver also resolved some of the noise on those channels. The knob redesign made it more secure, nonslip, and bump-free. Figure 3.1 shows the full design of the prototype device. Finally, when the control  $\text{FiO}_2$  is directed to increase or decrease the dial moves in respect to the position with some error and noise. This is seen in both Fig. 3.4 and Fig. 3.7, with the control  $\text{FiO}_2$  increasing while the measured  $\text{FiO}_2$  follows closely. An integral part of the design is that the  $\Delta\text{FiO}_2$  is needed for both the manual and automatic adjustments.

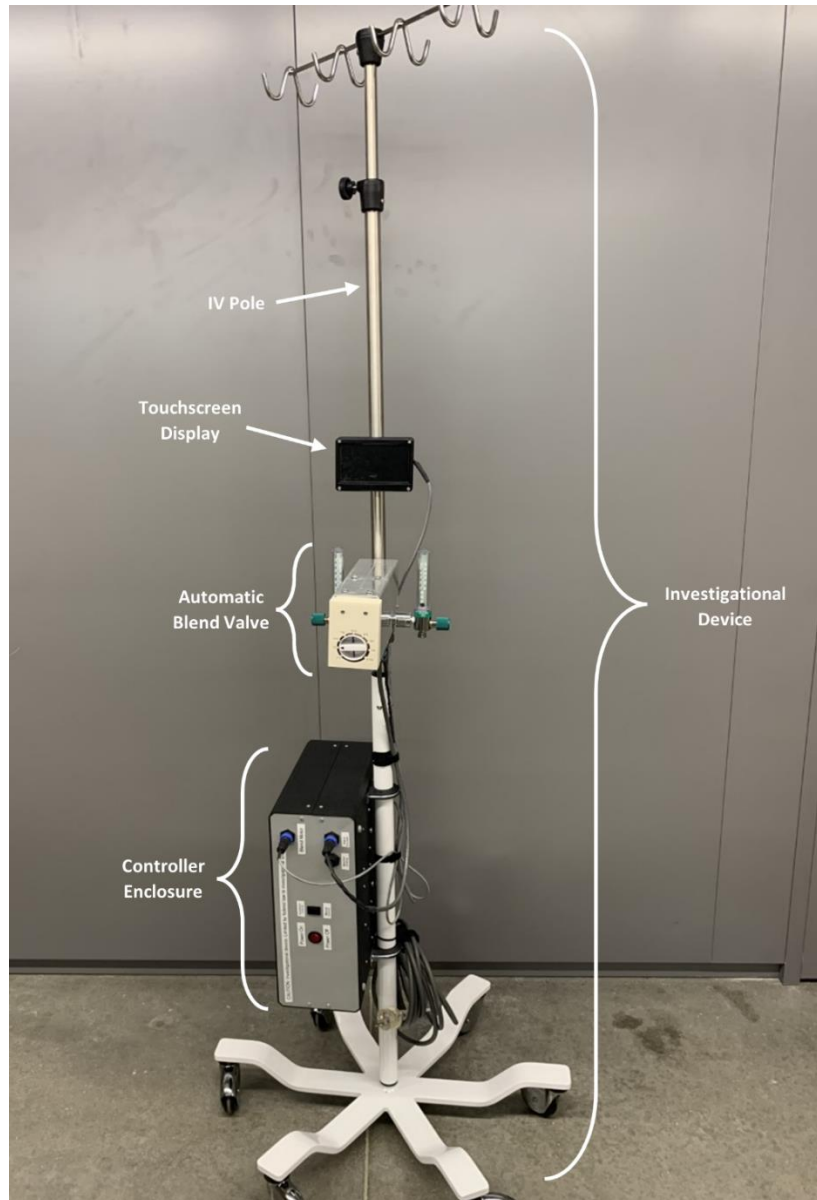


**Figure 3.1 Prototype device.**

### **3.2 Lab Testing Results**

Before clinical trials could be conducted, non-clinical testing was needed to compare the controller performance with the previous prototype. The Neonatal Respiratory System Simulator was used to compare the performance. The simulator receives the  $FiO_2$  signal from the oxygen analyzer and computes the  $SpO_2$  according to a previously developed dynamic model. Next, the

device generates the signal structure used by Spacelabs bedside monitors. The signal is then sent to the automatic oxygen control system in real-time. With this, the simulator is set up with  $G_p=3$  and time constant  $\tau=50$ , with an  $SpO_2$  disturbance of -3. This test would switch between manual and automatic control over the course of an hour. The test shows the system's response to repetitive and random  $SpO_2$  desaturation events. The switching between the two states allows the controller to respond to the input change and debug the system. The non-clinical data for the manual/auto switch test are given in Fig. 3.2, Fig. 3.3, and Fig. 3.4.

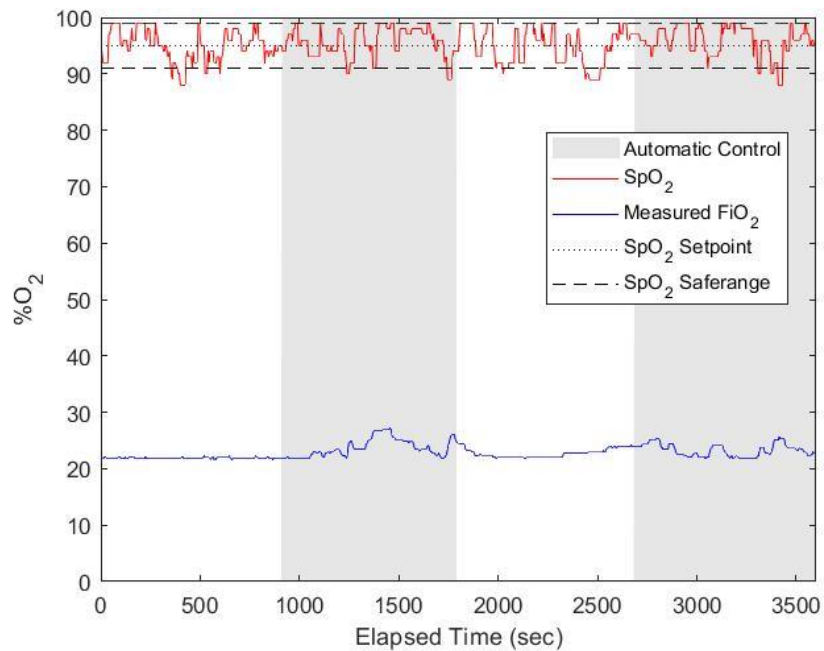


**Figure 3.2 Manual/Auto switch transition over an hour.**

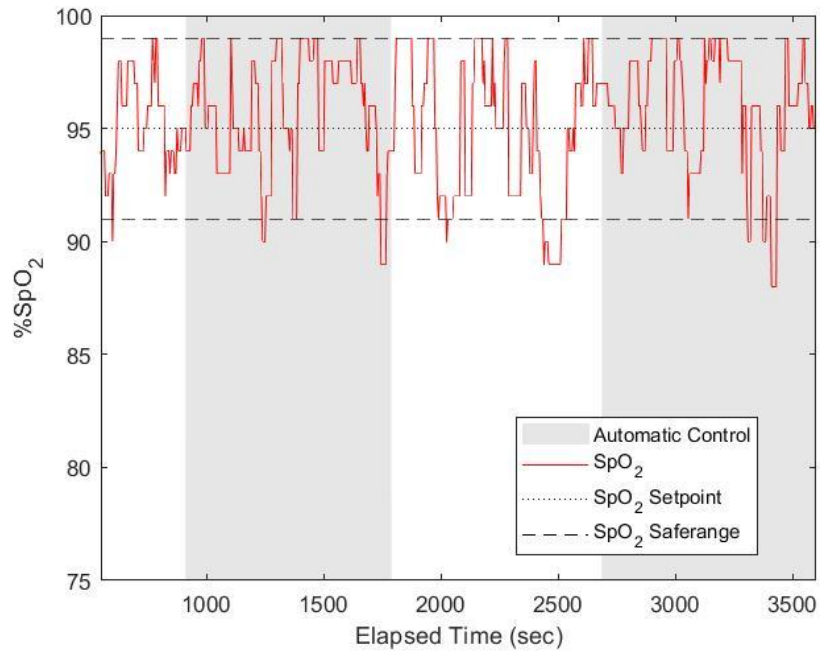


**Figure 3.3 Manual/Auto switch transition of SpO<sub>2</sub> over an hour**

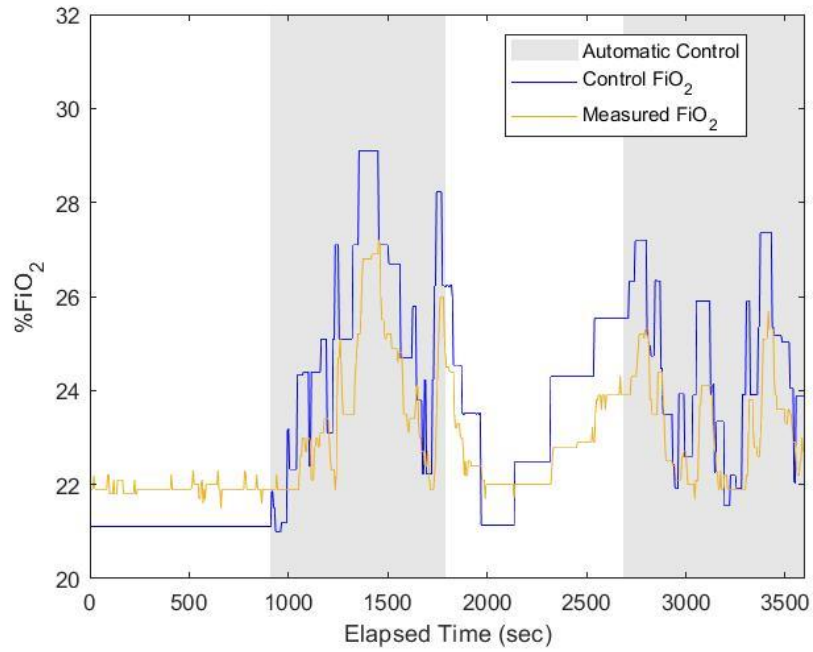


**Figure 3.4 Manual/Auto switch transition of FiO<sub>2</sub> over an hour**

**Table 3.1 Simulation results, percentage of time spent in each SpO<sub>2</sub> range in manual and automatic from the SpO<sub>2</sub> Setpoint**

	<b>Within 5 of the setpoint</b>	<b>Equal to the setpoint</b>	<b>Outside of 5 of the Setpoint</b>
<b>Manual (%)</b>	91.7%	3.1%	5.2%
<b>Automatic (%)</b>	94.7%	2.5%	2.8%

**Table 3.2 Simulation results, percentage of time spent in manual and automatic in each FiO<sub>2</sub> range**

	<b>Manual (%)</b>	<b>Automatic (%)</b>
<b>21~25</b>	100%	82.7%
<b>25~29</b>	0%	17.3%
<b>29~33</b>	0%	0%
<b>33~37</b>	0%	0%
<b>&lt;21 or &gt;37</b>	0%	0%

The second non-clinical test had similar parameters with a FiO<sub>2</sub> upper limit of 55%, a gain of  $G_p=3$ , time constant of  $\tau=50$ , and SpO<sub>2</sub> desaturation events at 700 seconds and 1200 seconds with corresponding disturbances of  $d(t)=-5$  and  $d(t)=-8$ , respectively. The simulated feeding process began at 1800 seconds and lasted for 1200 seconds. The SpO<sub>2</sub> levels were kept lower during the feeding process at an average value of 93%. The feeding process finished at 3000 s. The simulated non-clinical results are given in Fig. 3.5, Fig. 3.6, and Fig. 3.7.

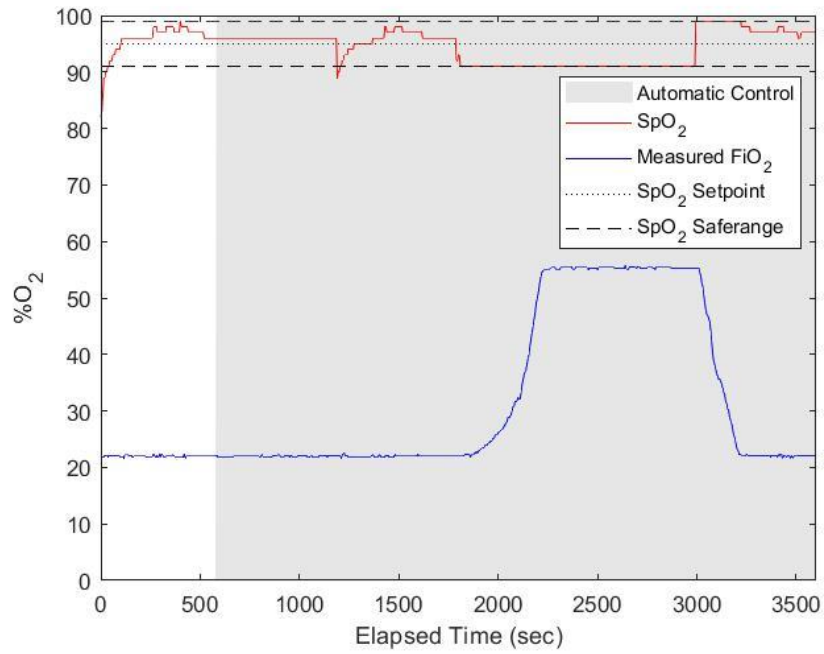


**Figure 3.5 Simulation desaturation and feeding test.**

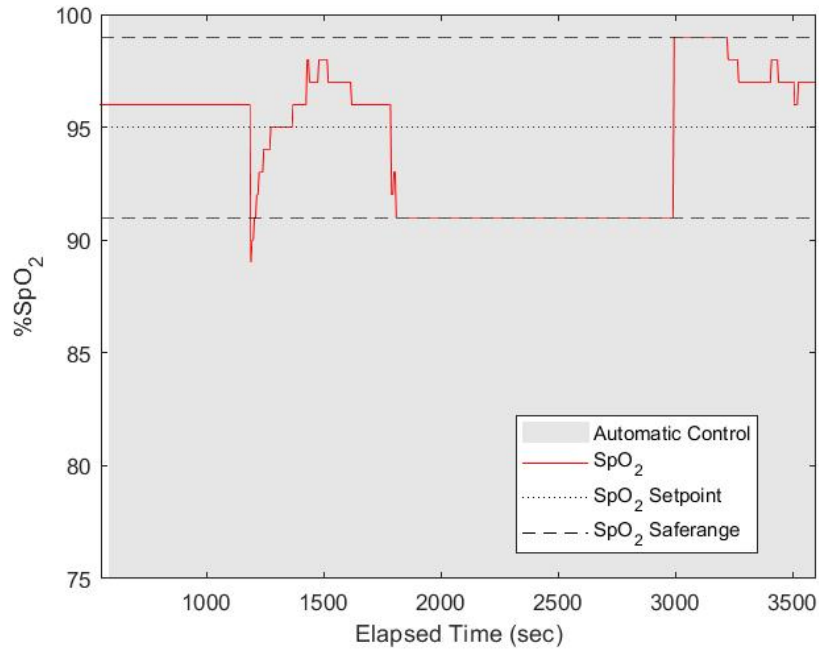


**Figure 3.6 Simulation desaturation and feeding test of SpO<sub>2</sub>.**

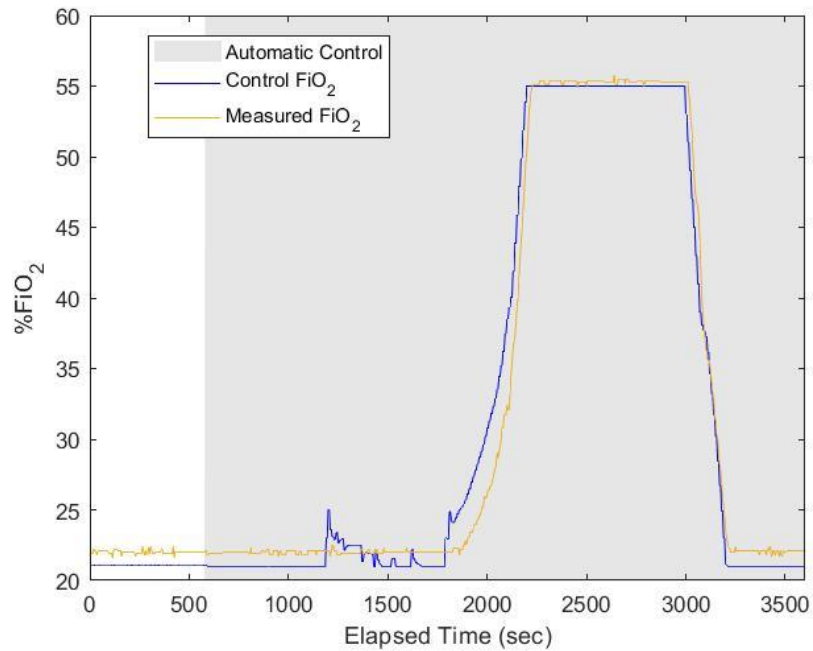


**Figure 3.7 Simulation desaturation and feeding test of FiO<sub>2</sub>.**

### 3.3 Clinical Trial Results

Clinical testing was conducted on three patients. The device was connected to a Spacelabs bedside monitor and an oxygen analyzer about 12 hours before the air lines were switched over. The start mode (auto/manual) would be randomized and unknown until the morning of the trial. The device would be switched every 6 hours thereafter. A research team member would sit at the bedside to monitor the device for the first 12 hours of runtime and return every day after that for one hour. The trial ran for six days. The setpoint of the SpO<sub>2</sub>, flow, and FiO<sub>2</sub> varied by patient based on specific patient needs. The results of the trial are presented in Table 3.1.

**Table 3.3 Clinical results from Subjects 1-3 by the percentage of time patients spent in a safe SpO<sub>2</sub> range**

<b>Subject</b>	<b>Automatic</b>	<b>Manual</b>	<b>Difference</b>
1	74.9%	66.6%	12.5%
2	78.5%	72.5%	8.3%
3	94.2%	94.5%	0.3%

Table 3.4 shows the resulting average of the subjects with percentage time running in manual and automatic mode in respect to the FiO<sub>2</sub> at incremented levels. Table 3.5 gives the average of the subjects with the percentage of time that the patients were in manual and automatic mode with respect to their SpO<sub>2</sub> levels being in a safe range. Lastly, the individual results for the three subjects are shown in Table 3.4 through Table 3.8.

**Table 3.4 Average of the subjects, percentage of time spent in manual and automatic in each FiO<sub>2</sub> range**

	<b>Manual (%)</b>	<b>Automatic (%)</b>
<b>21~25</b>	51.6%	53.9%
<b>25~29</b>	18.6%	22.0%
<b>29~33</b>	23.5%	16.3%
<b>33~37</b>	3.9%	5.0%
<b>&lt;21 or &gt;37</b>	2.4%	2.8%

**Table 3.5 Average of the subjects, percentage of time spent in each SpO<sub>2</sub> range in manual and automatic from the SpO<sub>2</sub> Setpoint**

	<b>Within 5 of the setpoint</b>	<b>Equal to the setpoint</b>	<b>Outside of 5 of the Setpoint</b>
<b>Manual (%)</b>	78.6	7.7	13.7
<b>Automatic (%)</b>	82.4	6.5	11.1

**Table 3.6 Patient 1's FiO<sub>2</sub> range in both modes in percent on time in each**

	<b>Manual</b>	<b>Automatic</b>
<b>21~25</b>	59.4%	65.1%
<b>25~29</b>	23.8%	16.1%
<b>29~33</b>	11.2%	8.1%
<b>33~37</b>	1.1%	4.6%
<b>&lt;21 or &gt;37</b>	4.5%	6.1%

**Table 3.7 Patient 1's SpO<sub>2</sub> range from the SpO<sub>2</sub> Setpoint in percent on time**

	<b>Manual</b>	<b>Automatic</b>
<b>Within 5 of the setpoint</b>	66.6%	74.9%
<b>Equal to the setpoint</b>	12.2%	9.5%
<b>Outside of 5 of the Setpoint</b>	21.2%	15.6%

**Table 3.8 Patient 2's FiO<sub>2</sub> range in both modes in percent on time in each**

	<b>Manual</b>	<b>Auto</b>
<b>21~25</b>	94.7%	91.4%
<b>25~29</b>	5.1%	6.3%
<b>29~33</b>	0.1%	1.4%
<b>33~37</b>	0.0%	0.4%
<b>&lt;21 or &gt;37</b>	0.1%	0.5%

**Table 3.9 Patient 2's SpO<sub>2</sub> range from the SpO<sub>2</sub> Setpoint in percent of time**

	<b>Manual</b>	<b>Automatic</b>
<b>Within 5 of the setpoint</b>	72.5%	78.5%
<b>Equal to the setpoint</b>	9.5%	7.8%
<b>Outside of 5 of the Setpoint</b>	18.0%	13.7%

**Table 3.10 Patient 3's FiO<sub>2</sub> range in both modes in percent on time in each**

	<b>Manual</b>	<b>Auto</b>
<b>21~25</b>	0.6%	5.3%
<b>25~29</b>	27.0%	43.7%
<b>29~33</b>	59.4%	39.4%
<b>33~37</b>	10.5%	9.8%
<b>&lt;21 or &gt;37</b>	2.5%	1.8%

**Table 3.11 Patient 2's SpO<sub>2</sub> range from the SpO<sub>2</sub> Setpoint in percent on time**

	<b>Manual</b>	<b>Automatic</b>
<b>Within 5 of the setpoint</b>	94.5%	94.2%
<b>Equal to the setpoint</b>	2.2%	1.9%
<b>Outside of 5 of the Setpoint</b>	3.3%	3.9%

### **3.4 Discussion**

This chapter discusses the results of the clinical device design, non-clinical testing, and clinical trials. In addition, it examines whether the device's performance met or exceeded the system's requirements while also keeping the neonate's SpO<sub>2</sub> levels in a safe range. The efficiency of nurses interacting with the device according to proper protocols was also demonstrated.

The resulting design of the device is shown in Fig 3.1 with all incorporated requirements, along with room to expand. DFM was followed in the design and development of the prototypes to create repeatability throughout each step of the process. This allows for both additive and subtractive manufacturing of components. With the use of standard wiring such as T568B for

RJ45 connectors, T568B to DB9 connectors, and then using the same four pin four wire connectors for the motor driver, motor encoder, and the Masimo pulse oximeter (not used at this time) to have a standard design that is repeatable. While the design has been improved, the connector to both the motor and the encoder could have disconnects attached to the housing of the blend valve assembly. This would benefit both the blend valve assembly in manufacturing and the wiring needed to be run to them. When developing the prototypes, both the sbRIO-9627 and sbRIO-9628 were needed to test both platforms, but chip shortages and defective components among the two sbRIO-9627 boards and similar defects with another two sbRIO-9628 boards would not allow for full utilization of the boards.

Lab testing closely followed previous researchers' non-clinical device testing. During the monitoring period, several changes to the initial design were performed. One-megaohm pull-down resistors were placed in four locations to lessen the noise on those channels. A pull-down resistor on the manual/auto switch increased the reliability of the switch. Furthermore, issues with the blend valve assembly would be addressed for both functionality and user interaction. Results from lab testing shown in Fig. 3.2 through Fig. 3.4 demonstrate that changing between manual and automatic modes results in a smooth transition for  $\text{FiO}_2$  adjustments where the blend servo motor does not cause the motor to react erratically. The results in Fig. 3.5 through Fig. 3.7 demonstrate the tests run to validate the systems previously developed by researchers. The results showed that the device has smooth responses to desaturate events while not exceeding the set threshold. These findings follow closely with the results presented by Hou.

Clinical results presented in Table 3.1 through Table 3.3 give the average test results from the first three subjects in the trial. The results show that there is a difference between the two operations modes with a slight advantage to the automatic mode in keeping the  $\text{SpO}_2$  within

the safe range. Furthermore, the data in Table 3.2 reveals that the device being ran in manual or automatic mode kept the  $\text{FiO}_2$  in the same range spectrum. Looking further into the data from each subject in Table 3.4 through Table 3.9, the findings show that in Subject One, the neonate is kept in a safe  $\text{SpO}_2$  range longer when in automatic mode than in manual, which is also the case for Subject Two. However, the results for keeping the patient in the safe  $\text{SpO}_2$  range are almost identical in Subject Three. This leads to the data on the percentage of time the patient is in each  $\text{FiO}_2$  range. Results for Subject One show that the patient was kept in the 21%~25%  $\text{FiO}_2$  range longer in automatic mode than in manual mode while also staying in a safe range for their  $\text{SpO}_2$  levels. This trend is similar in Subject Two, as the  $\text{SpO}_2$  safe range results show a slight advantage to the automatic mode, with the  $\text{FiO}_2$  results showing a slight variance in the  $\text{FiO}_2$  being supplied. The result suggests that the device is responding well to desaturation events. Along with the results from Subject Three having the  $\text{SpO}_2$  data being so close in both modes, the  $\text{FiO}_2$  data shows that while in automatic mode, the  $\text{FiO}_2$  was kept at a lower range, while meeting the same percentage of  $\text{SpO}_2$  results in manual mode. From the first three subjects, the data presented shows that the device runs similarly to the nurse's interaction in the early trial.

#### 4. Conclusion and Future Work

Infants admitted to the NICU are currently being placed on respiratory support devices that nurses operate. These nurses have dynamic workloads and must manually adjust the  $\text{FiO}_2$  supplied to the infant based on its  $\text{SpO}_2$  levels; these conditions can lead to very high  $\text{SpO}_2$  levels, which risk retinopathy of prematurity (ROP), and low  $\text{SpO}_2$ , which can lead to brain damage and even death. The work in this paper explains the implementation of Pierce's redesigned blend valve assembly with the new CompactRIO using the same control algorithm designed by Kiem and Krone. The paper's main topics focused on implementing the new automatic blend valve assembly with the new CompactRIO, along with the design for manufacturing and the reliability of the new system in lab testing and in clinical testing.

While following the basic DFM, the use the same components to minimize the number of different connectors, the use of different types of wires for different applications and simplifying the layout of the CompactRIO enclosure to allow for less manufacturing processes to be designed and a less complex assembly process. Following that is the investigation into the sbRIO-9627 and sbRIO-9628 for stability and reliability with the other components. Preliminary testing was then completed for the CompactRIO, analyzing the serial ports, digital ports, analog ports, and the overall function of the units. Through these tests, manufacturing flaws that were not caught by the quality control department were found and addressed. The boards that passed the preliminary tests went on to lab testing and clinical testing. With the testing of the sbRIO-9628, the board is found to be reliable and stable when all preliminary testing of the CompactRIO tests correctly. The sbRIO-9627 did not get to be thoroughly tested because a functioning CompactRIO that passed all preliminary testing was never received. However, with the similarities between the boards, the use of the sbRIO-9627 could be concluded if the

CompactRIO passed preliminary testing. Finally, the design was tested successfully in the clinical environment with better results for automatic operation over manual due to the implementation of the hardware and software design.

In future work the performance of the original CompactRIO, sbRIO-9632 can be adapted to run the control system. However, support for the unit has been discontinued by the manufacturer. The search for a reliable CompactRIO has dwindled along with the chip shortage. Further testing into the use of microcomputers with the use of data acquisition units or USB FPGA cards should be considered. Early testing of these systems has proven to be reliable.

## References

- [1] Keim, T., Amjad, R., and Fales, R., "Modeling and Feedback Control of Inspired Oxygen for Premature Infants," Proc. ASME 2011 Dynamic Systems and Control Conference and Bath/ASME Symposium on Fluid Power and Motion Control, American Society of Mechanical Engineers.
- [2] Keim T., "Control of Arterial Oxygen Saturation in Premature Infants," Thesis, University of Missouri-Columbia, 2011.
- [3] Keim, T., Amjad, R., and Fales, R., "Modeling and control of the oxygen saturation in neonatal infants," Proc. ASME 2009 Dynamic Systems and Control Conference, American Society of Mechanical Engineers, pp. 105-112.
- [4] Krone, B., Fales, R., and Amjad, R., "Model of Neonatal Infant Blood Oxygen Saturation," Proc. ASME 2011 Dynamic Systems and Control Conference and Bath/ASME Symposium on Fluid Power and Motion Control, American Society of Mechanical Engineers, pp. 509-516.
- [5] Krone, B., 2011, "Modeling and control of arterial oxygen saturation in premature infants," University of Missouri-Columbia.
- [6] D. Quigley, "Control of arterial hemoglobin saturation in premature infants using H-infinity synthesis and performance specifications from best clinical practice," M.S., University of Missouri--Columbia, 2013
- [7] Alkurawy L., "Design of an Efficient Controller for Arterial Oxygen Saturation in Neonatal Infants", University of Missouri- Columbia
- [8] Faqeeh, A., Hou, X., Zaniletti, I., Pardalos, J., Amjad, R., and Fales, R., 2018, "Comparison of Automated and Manual Peripheral Oxygen Saturation Control Applied to One Human Subject at a High Target Range," Conf Proc IEEE Eng Med Biol Soc, 2018, pp. 3346-3349.
- [9] Faqeeh, A., Fales, R., Pardalos, J., Amjad, R., Zaniletti, I., and Hou, X., 2018, "Engineering Evaluation of the Performance of an Automatic Peripheral Oxygen Controller Using a Neonatal Respiratory Model," Journal of Medical Devices, 12(3), p. 031005
- [10] Faqeeh, A. A. A., 2018, "Investigation of the performance of an automatic arterial oxygen controller," Doctor of Philosophy, University of Missouri, Columbia, MO.
- [11] Stuarts B., "Parameterized Uncertainty Modeling Applied to the Oxygen Control of Neonates with Lung Disease", University of Missouri- Columbia
- [12] Hou, X., Faqeeh, and Fales, R., "Automatic Oxygen Controller Design for Premature Infants with Clinical Evaluation", University of Missouri-Columbia

- [13] Hou, Xuefeng, et al. “Clinical Evaluation of an Automatic Oxygen Control System for Premature Infants Receiving High-Flow Nasal Cannula for Respiratory Support: A Pilot Study.” *Journal of Medical Devices*, vol. 16, no. 3, Sept. 2022, p. 031005. *EBSCOhost*, <https://doi.org/10.1115/1.4054250>.
- [14] R. Dutton, “Polynomial System Identification Modeling and Adaptive Model Predictive Control of Arterial Oxygen Saturation in Premature Infants,” MS, University of Missouri—Columbia, 2020.
- [15] Pierce E., and Roger Fales, “Design of a simple Drive Train and Control System for an oxygen Blend Valve for use with Premature Infants”, University of Missouri- Columbia
- [16] Maj P., “1.2 Mfps standalone X-ray detector for Time-Resolved Experiments”, *Journal of Instrumentation*.2020.
- [17] “Product documentation,” *NI* Available: <https://www.ni.com/docs/en-US/bundle/sbriio-9628-specs/page/specs.html>.
- [18] BIO MED BLEND VALVE MANUAL
- [19] SOLA/HEVI-DUTY, *SCP-Manual*, n.d..
- [20] Reach Technology Inc., “SLCD43 Controller Manual V1.26 Hardware Revisions A, B, H01 and H02” 04/20/2015